MOLECULAR AND CELLULAR BIOLOGY, Aug. 2007, p. 5711–5724 Vol. 27, No. 16
0270-7306/07/$08.00+0 doi:10.1128/MCB.00482-07
Copyright © 2007, American Society for Microbiology. All Rights Reserved.

SET8-Mediated Methylations of Histone H4 Lysine 20 Mark Silent Heterochromatic Domains in Apicomplexan Genomes▽†

Céline F. Sautel,[1] Dominique Cannella,[1] Olivier Bastien,[1] Sylvie Kieffer,[4] Delphine Aldebert,[1] Jérôme Garin,[4] Isabelle Tardieux,[3] Hassan Belrhali,[2] and Mohamed-Ali Hakimi[1]*

UMR5163/CNRS-Joseph Fourier University, Jean-Roget Institute, Grenoble F-38042, France[1]; EMBL-Grenoble Outstation, Grenoble F-38042, France[2]; Institut Cochin, Paris F-75014, France[3]; and INSERM ERIT, M 0201, CEA, Grenoble, France[4]

Received 20 March 2007/Returned for modification 3 May 2007/Accepted 5 June 2007

Posttranslational histone modifications modulate chromatin-templated processes in various biological systems. H4K20 methylation is considered to have an evolutionarily ancient role in DNA repair and genome integrity, while its function in heterochromatin function and gene expression is thought to have arisen later during evolution. Here, we identify and characterize H4K20 methylases of the Set8 family in *Plasmodium* and *Toxoplasma*, two medically important members of the protozoan phylum *Apicomplexa*. Remarkably, parasite Set8-related proteins display H4K20 mono-, di-, and trimethylase activities, in striking contrast to the monomethylase-restricted human Set8. Structurally, few residues forming the substrate-specific channel dictate enzyme methylation multiplicity. These enzymes are cell cycle regulated and focally enriched at pericentric and telomeric heterochromatin in both parasites. Collectively, our findings provide new insights into the evolution of Set8-mediated biochemical pathways, suggesting that the heterochromatic function of the marker is not restricted to metazoans. Thus, these lower eukaryotes have developed a diverse panel of biological stages through their high capacity to differentiate, and epigenetics only begins to emerge as a strong determinant of their biology.

The fundamental unit of chromatin, termed the nucleosome, is subject to a dizzying array of posttranslational modifications, which work alone or in combination to constitute a histone code that regulates chromatin structure and function (18). Among these modifications, lysine methylations index chromatin regions, facilitating epigenetic organization of eukaryotic genomes. In contrast to other histone-modifying enzymes, *h*istone lysine (*K*) *m*ethyl*t*ransferases (HKMTs) are enzymes devoted to the methylation of highly specific lysine residues which either promote gene activation (H3K4, H3K79, and H3K36) or generate a repressed chromatin state (H3K9, H3K27, and H4K20). With just one exception (Dot1p), these enzymes belong to the SET family. The SET domain, which initially took its name from the *Drosophila* genes *S*u(var)3-9, *e*nhancer of zeste, and *t*rithorax, is crucial for the catalytic activity of HKMTs (3, 9, 24). While lysine methylation mainly occurs on histone H3 tails, the only lysine residue of histone H4 shown to be methylated in vivo is lysine 20. Methylation of H4K20 is involved in a diverse array of nuclear processes, including gene silencing (12, 26), pericentric heterochromatin formation (37), mitotic regulation in metazoans (20, 21), and DNA damage checkpoint control in the cell cycle of *Schizosaccharomyces pombe* (35).

A number of different SET proteins have been identified as being able to methylate H4K20, including metazoan Set8 (also named Pr-Set7) (12, 26), *Drosophila* ASH1 (2), murine NSD1 (30), mammalian SUV4-20H1/2 (37), and its *S. pombe* ortholog SET9 (35). The modification is evidently absent in several simple eukaryotes, such as *Saccharomyces cerevisiae* and the ciliated protozoan *Tetrahymena thermophila* (26). H4K20 methylation by SET9 was, however, reported in *S. pombe*, where it does not act on the regulation of gene expression or heterochromatin function but is instead required for the recruitment of the checkpoint protein Crb2 to sites of DNA damage (35). Thus, the role of H4K20 methylation in DNA repair and genome integrity can be considered an early evolutionary function whereas the heterochromatin function of the marker arose later in evolution in response to increasing genome complexity. This argument prompted us to look for the presence of the marker (H4K20 methylation) in early-branching eukaryotic cells within the *Apicomplexa* phylum.

Apicomplexa is a phylum of unicellular parasites that includes important human pathogens like *Plasmodium* species, the causative agents of malaria, and *Toxoplasma gondii*, a common cause of congenital ocular and cerebral diseases, as well as of severe encephalitis in immunocompromised individuals. An obligatory intracellular lifestyle has been adopted by these parasites as a successful immune evasion mechanism. As a consequence, they have evolved a number of properties that allow them to survive and grow under several host cell conditions throughout their life cycle. The development of several biological stages that express different sets of genes following a differentiation phase has been key in their success. These parasites possess a rich but still largely unexplored repertoire of enzymes the functions of which are associated with epigenetics and chromatin remodeling. These processes are expected to be extensively used given the multiple life cycle stages of these parasites (11, 13, 34, 41).

* Corresponding author. Mailing address: Epigenetic and Parasites ATIP Group, UMR5163, LAPM, Institut Jean Roget, BP 170, 38042 Grenoble Cedex 9, France. Phone: (33) 4 76 63 74 69. Fax: (33) 4 76 63 74 97. E-mail: Mohamed-Ali.Hakimi@ujf-grenoble.fr.

† Supplemental material for this article may be found at http://mcb.asm.org/.

▽ Published ahead of print on 11 June 2007.

Downloaded from mcb.asm.org at SISTEMA INTEGRADO DE BIBLIOTECAS DA USP on September 6, 2007

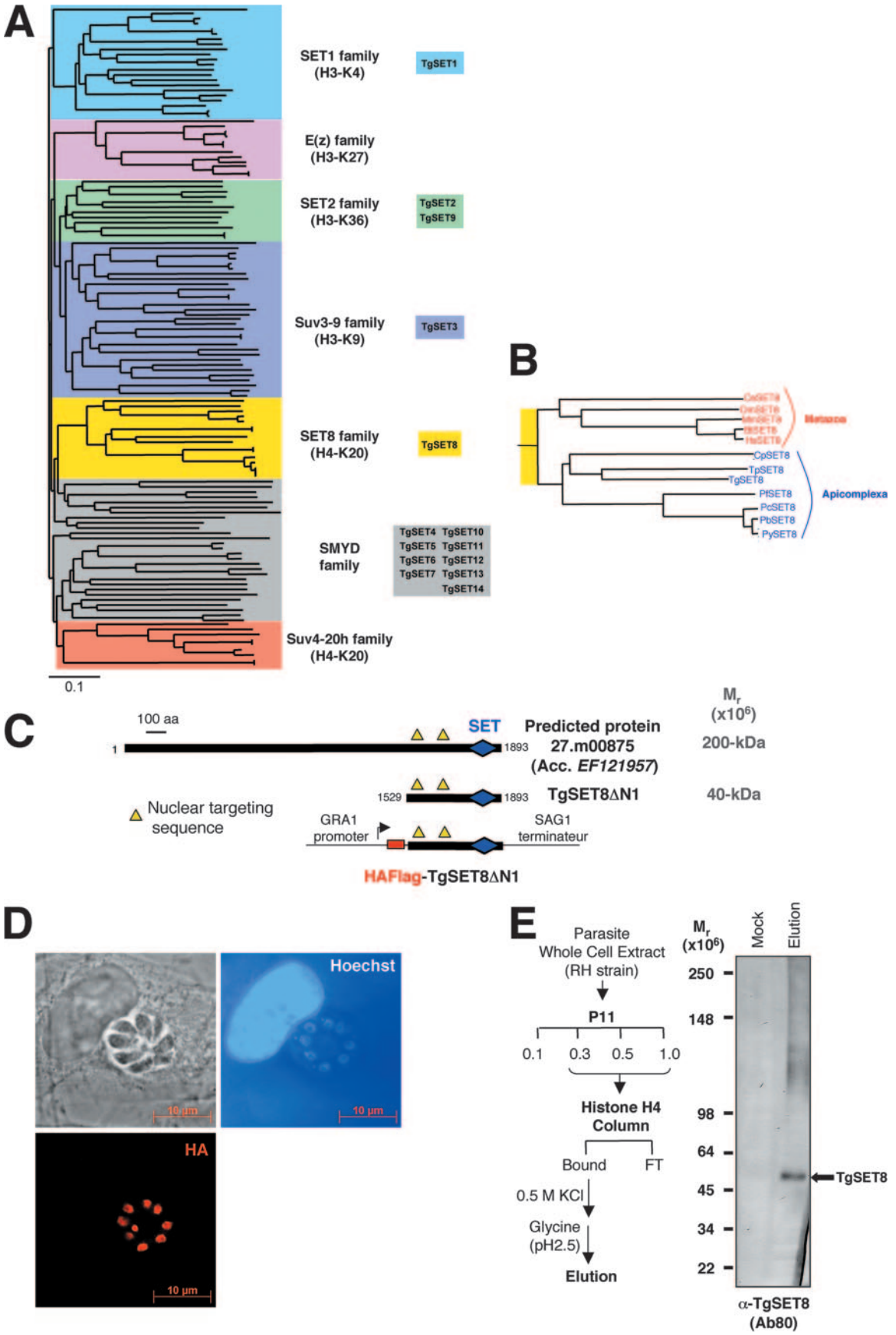

Downloaded from mcb.asm.org at SISTEMA INTEGRADO DE BIBLIOTECAS DA USP on September 6, 2007

In this report, we first describe the identification and functional analyses of a novel apicomplexan family of histone methyltransferases (HMTases) specific for H4K20 methylation. Unexpectedly, we identified parasite proteins with significant matches to human Set8, while no Suv4-20 h orthologs were found. Even more surprising, biochemical and structural modeling analyses demonstrated that *T. gondii* Set8 (TgSet8) can transfer mono-, di-, and trimethyl H4K20 sequentially, whereas its human counterpart is exclusively found as a monomethylase. Additionally, TgSet8 and the monomethylated marker are cell cycle regulated. Importantly, we established by chromatin immunoprecipitation (ChIP) that both TgSet8 and the repressive methylation markers on H3K9 and H4K20 are localized at heterochromatic domains such as silenced rRNA gene, satellite repeat, and telomeric regions. Collectively, our findings provide new insights into the evolution of Set8-mediated biochemical pathways, suggesting that the heterochromatic function of the marker is not restricted to metazoans.

MATERIALS AND METHODS

Parasite methods. Standard laboratory methods and techniques for *T. gondii*, *Neospora caninum*, and *Plasmodium* sp. manipulations were used. RH strains of *Toxoplasma* were grown in human foreskin fibroblasts, transfected, and cloned by limiting dilution as described previously (34). The *RHhxgprt* mutant strain used in these studies contains a defective hypoxanthine-guanine-phosphoribosyltransferase (*HXGPRT*) gene or lacks the gene, which allows the selection of transfected tachyzoites with mycophenolic acid (10).

Immunofluorescence assay and Western blot analysis. Immunofluorescence assays and immunoblotting with alkaline phosphatase was performed as described previously (34).

In vitro HMTase assay. Recombinant protein rTgSET8ΔN1 and its derivatives were purified from bacteria as described previously (34). Histidine-tagged histone H4 was purified from bacteria as described previously (42). Core histones and mononucleosomes were extracted from tachyzoites (*T. gondii* strain RH). Protein samples (rTgSET8, rTgSET8 mutant forms, Suv4-20h1, or PrSET7) were incubated with recombinant histone H4 or free core histones at 30°C for 60 min in methyltransferase buffer (final concentrations, 50 mM Tris-HCl [pH 8.5], 0.5 mM dithiothreitol, and 1 mM phenylmethylsulfonyl fluoride) and 0.1 mM *S*-adenosyl-L-methionine (Sigma) as previously described. The reaction was stopped by addition of sodium dodecyl sulfate (SDS) sample buffer, and the reaction mixtures were analyzed by 10% to 20% gradient SDS-polyacrylamide gel electrophoresis, followed by Western blotting with antibodies to H4K20me1 (39), H4K20me2 (39), and H4K20me3 (ab9053; Abcam).

RESULTS

Identification of a new family of HMTase related to human Set8 in apicomplexan parasites. The SET domain is likely to have arisen early in eukaryotic evolution. The domain is present in multiple copies in all currently available eukaryotic proteomes, including all of the crown group taxa, and various earlier diverging protist lineages (1). Phylogenetic analysis indicates that there was significant duplication and divergence of SET domain proteins in the *Apicomplexa* lineage. Surprisingly, a survey of available genomic databases indicates that Set8 homologs arose predominantly in all of the *Apicomplexa* members examined so far, suggesting that this orphan member is not restricted to metazoans, as previously thought (Fig. 1A and B, yellow colored). Intriguingly, no homologs were found in ciliates (26) and dinoflagellates although there is a great deal of sequence information available for the large clade of *Alveolata*, which contains the ciliates, dinoflagellates, and apicomplexans. Absence of Set8 in ciliates can be explained by subsequent loss of the gene for Set8 in that lineage. This is a common phylogenetic occurrence; for example, dinoflagellates, which are frequently considered relatives of *Apicomplexa*, have lost histones altogether (15). This apparent paradox can be alternatively explained by a lateral genetic transfer during which the apicomplexan ancestor acquired a Set8-related gene from a host belonging to the animal lineage. Such a transfer is highly supported by the intracellular location of apicomplexan parasites for most of their life cycle, and it has been already exemplified with other apicomplexan proteins characterized as reminiscent of animal proteins (27, 43).

The predicted *TgSet8* gene (27.m00875; http://ToxoDB.org) encodes a predicted protein of 1,893 amino acids (202 kDa) that harbors a conserved C-terminal SET domain (Fig. 1C). However, biochemical purification shows the appearance of a single polypeptide of approximately 55 kDa (Fig. 1E), suggesting that the product of 27.m00875 was mispredicted. We then cloned a partial-length cDNA encoding the C-terminal domain of the protein and encompassing both putative nuclear localization signals (TgSet8ΔN1 amino acid residues 1529 to 1893; 40-kDa). We consider here that the recombinant TgSet8ΔN1 is almost equivalent to the native protein. Immunofluorescence analysis of stable transgenic parasites (strain RH) ectopically expressing recombinant TgSet8ΔN1 dually tagged with hemagglutinin (HA) and Flag verifies the exclusive nuclear localization of TgSet8 (Fig. 1D). Multiple attempts to generate a knockout of the *TgSet8* gene failed, suggesting that the gene may be essential in tachyzoites (data not shown).

TgSet8 defines a new family of HKMTs that mono-, di-, and trimethylate lysine 20 of histone H4. To begin defining the role of TgSet8, we initially asked whether or not histone H4 is methylated at lysine 20 in *T. gondii*. Immunoblotting with a panel of H4K20 methyl-specific antibodies showed that native histone cores were specifically mono-, di-, and trimethylated (Fig. 2A; see Table S2 in the supplemental material). We therefore hypothesize that TgSet8 is inherently involved in H4K20 methylation. Recombinant TgSet8ΔN1 purified from *Escherichia coli* methylated only histone H4 (as free histone) and not H2A, H2B, or H3, indicating that TgSet8ΔN1 has intrinsic HMTase activity and retains its substrate specificity (Fig. 2C). As lysine 20 can be mono-, di-, or trimethylated, we

FIG. 1. A new SET8 family. (A) Schematic dendrogram showing the relationships among some of the better-characterized SET domain proteins. For a more detailed phylogenetic tree, see Fig. S1 in the supplemental material. Major lineages of the SET domain and *T. gondii* TgSet proteins are indicated next to the tree. (B) Expanded representation of the new SET8 family branch. (C and D) Costaining with anti-HA antibody and Hoechst 33258 of human fibroblast cells infected with transgenic *T. gondii* strain RH::HA-Flag–TgSet8. The transgene is driven by the parasite-specific strong promoter *GRA1*. aa, amino acids; Acc., accession no. (E) *T. gondii* whole-cell extract was fractionated by chromatography, and the fraction shown by an arrow was used for histone H4 affinity purification, followed by Western blotting with a specific antibody raised against TgSet8.

Downloaded from mcb.asm.org at SISTEMA INTEGRADO DE BIBLIOTECAS DA USP on September 6, 2007

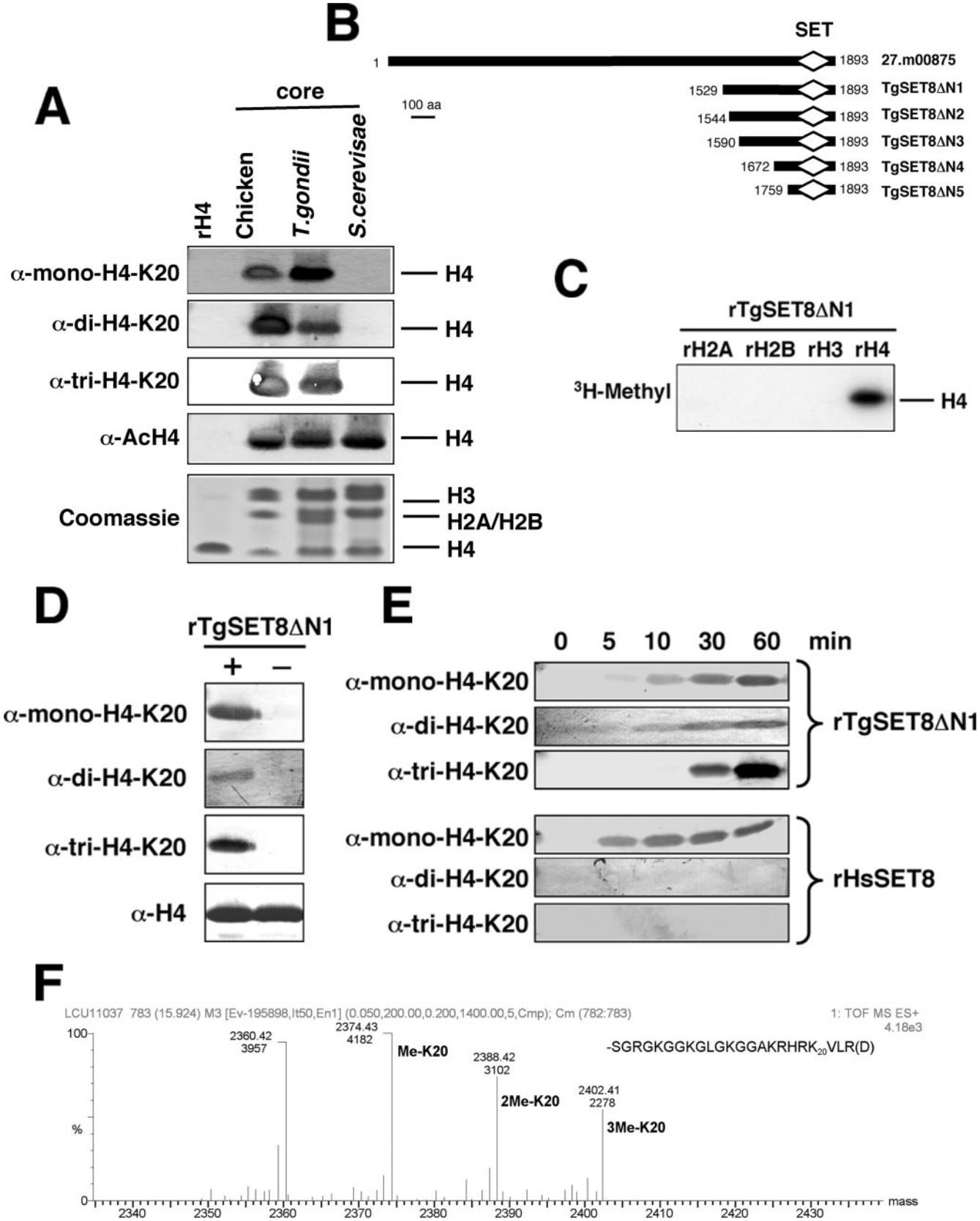

FIG. 2. Methylation of *T. gondii* H4K20 is mediated by TgSet8. (A) Histones were extracted from the indicated organisms and fractionated by SDS-polyacrylamide gel electrophoresis. (Top) Western blot analysis with antibodies against H4K20me1 (39), H4K20me2 (Ab1, Upstate 07-441; Ab2, reference 39; Ab3, Abcam ab9052), H4K20me3 (Abcam ab9053), and unmodified histone H4 (Abcam ab4559). (Bottom) Coomassie staining

Downloaded from mcb.asm.org at SISTEMA INTEGRADO DE BIBLIOTECAS DA USP on September 6, 2007

next investigated the methylation state of the TgSet8ΔN1 reaction products. First, we showed a clear enrichment for H4K20me1 but also di- and trimethylation of the residue (Fig. 2D). This result was unexpected since the mammalian counterpart, Set8, is known to catalyze H4K20me1 exclusively (8, 46, 47). Secondly, the kinetics of the TgSet8ΔN1 products show that while H4K20me1 increased over time—as for its human counterpart—TgSet8ΔN1 remarkably displayed a direct progression to H4K20me3 with a relative accumulation of dimethyl products (Fig. 2E). To confirm the product specificity of rTgSet8ΔN1, we conducted HMTase assays and subjected aliquots of the reaction mixture to mass spectrometry to determine the methylation state of lysine 20 in recombinant histone H4. The data indicate a shift in the mass/charge (*m*/*z*) ratio of the digested H4 peptide from 2,360 (unmethylated) to 2,374 (one methyl), 2,388 (two methyls), and 2,402 (three methyls) (Fig. 2F). Thus, rTgSet8ΔN1 is a bona fide histone H4K20 mono-, di-, and trimethylase. A key question remains what the structural basis of TgSet8 substrate specificity and methylation multiplicity is.

Mutation V1875Y at the catalytic site of TgSet8 ablates trimethylase activity. The active-site architecture is strongly conserved between TgSet8 and HsSet8, allowing us to use the HsSET8 structure (1zkkA) in complex with the histone H4 10-residue peptide and the *S*-adenosyl-L-homocysteine (SAH) methyl donor cofactor product moiety to model a TgSet8ΔN5-SAH-lysine 20 complex (Fig. 3C and D). The HsSet8 lysine-binding pocket walls are mainly formed by two sequence stretches, Cys270 to Tyr274 and Tyr334 to Tyr336. Tyr245 is located at the distal end of the pocket, where lysine 20 is bound in an extended all-*trans* conformation and His18 of the peptide substrate is closing the top of the cavity. The TgSet8ΔN5 lysine-binding pocket residues are either strictly conserved (Tyr245 and Tyr336 in HsSet8, corresponding, respectively, to Tyr1779 and Tyr1877 in TgSet8) or changed to space-filling analogs, i.e., Tyr271 and Tyr273 in HsSet8, corresponding to Phe1806 and Phe1808 in TgSet8, respectively (Fig. 3C and D).

The only and noticeable exception is the HsSet8 Tyr334 amino acid, which becomes Val1875 in TgSet8. This substitution widely opens the K20 imidazole group binding pocket (Fig. 3D) and, together with the Tyr-to-Phe double substitutions described above, makes the pocket largely hydrophobic. It is interesting, moreover, that Phe1806 partially fills the hole created by the tyrosine-to-valine (1875) substitution in TgSET8 and also enforces the hydrophobic character of the K20 imidazole group binding site (Fig. 3D). *Neurospora crassa* DIM-5 histone H3-K9 trimethyltransferase has been structurally characterized in complex with the SAH cofactor product and the K9 peptide (48). Comparison of the DIM-5 and HsSet8 active sites also reveals hydrophobic substitutions, namely, Tyr273 to Phe206 and Tyr334 to Phe281 (Fig. 3D).

Changing Val1875 to a tyrosine in TgSet8 was then expected to lead to a narrowed and polar active-site distal extremity, as in the case of HsSet8, and hence to reduced trimethylase activity. Interestingly, time course experiments indicated that the reaction by V1875Y stalled at the mono- and dimethyl stage, while H4K20me3 still increased over time for the wild-type enzyme (Fig. 4B). Remarkably, the V1875Y mutation changed the product specificity of TgSet8 from a fast mono- or trimethyltransferase to a predominantly mono-HMTase with a slow dimethyltransferase activity without affecting its overall catalytic activity. Similarly, while *Neurospora* DIM-5 generates primarily H3K9me3, the mutation F281Y confines the enzyme to mono- and dimethylation (49). Likewise, mammalian G9a is converted from a fast mono- or di-HMTase with slow tri-HMTase activity to a predominantly mono-HMTase by the F1205Y mutation (6).

F1808Y mutation in the catalytic site unbalances the ratio of mono- to trimethylation. Several structural studies have shown that a conserved Tyr or Phe residue within the SET domain could be the key determinant specifying whether a SET domain catalyzes mono-, di-, or trimethylation (28). We noticed that a change of Phe to Tyr at position 1808 drastically enhanced trimethylation activity in vitro (Fig. 4C). Time course experiments showed that the trimethylated forms accumulate earlier in the reaction for the TgSet8ΔN1(F1808Y) mutant than for the wild type (2 min versus 30 min, respectively; Fig. 4B to D). Additionally, the yield of monomethylation decreased considerably in the reaction catalyzed by the mutated protein, whereas dimethylation increased significantly. Remarkably, the F1808Y mutation confines the enzyme in vitro to mediating trimethylation.

In light of the modeling that clearly reveals a wider and more hydrophobic lysine binding site, we have modeled the F1808Y substitution of TgSET8 (Fig. 4, compared panels A and C). This mutation is located right at the pocket entrance and more than 8 Å away from the lysine amine group. This reduced lysine channel diameter might make it more difficult for the lysine to enter but also more difficult for it to exit. Moreover, the Tyr1808 hydroxyl group does not face any proton acceptor in the protein active site; hence, it might be able to interact with the peptide substrate, increasing the binding of the TgSET8 mutant with the histone tail. We then hypothesized that after entering and being monomethylated, the lysine amine group has plenty of space to reposition itself so that it gets di- and trimethylated sequentially. The F1808Y mutation would make protein-histone tail binding tighter and, at the same time, sterically more difficult to dissociate by reducing

of histones. AcH4, acetylated H4. (B) Schematic representation of N-terminal deletion mutant forms of TgSet8. The amino acid (aa) numbers for each construct and the SET domain are indicated. (C) HMTase assays with TgSet8ΔN1 following incorporation of ^{3}H-labeled CH_3 into recombinant histone substrates rH3, rH4, rH2A, and rH2B. (D) HMTase assays of TgSet8ΔN1 with recombinant His_6-H4 were analyzed by Western blotting. No cross-reaction with recombinant H4 was observed. (E) Time course HMTase assays of TgSet8ΔN1 and rHsSet8 (Upstate). Reactions of TgSet8ΔN1 or rHsSet8 with recombinant His_6-H4 were stopped at sequential incubation time points and analyzed by Western blotting. (F) Product specificity of rTgSet8ΔN1 determined by mass spectrometry. Deconvoluted electrospray mass spectrum of the SGRGKGG KGLGKGGAKRHRK$_{20}$VLR(D) peptide following AspN digestion as described in Materials and Methods. The molecular masses of the unmethylated and mono-, di-, and trimethylated peptides are marked above the peaks. (G) Gel filtration chromatographic analysis of recombinant TgSet8ΔN1 with a Superdex 200 column. The eluted fractions were analyzed by Coomassie staining, Western blot analysis, and HMTase assay.

Downloaded from mcb.asm.org at SISTEMA INTEGRADO DE BIBLIOTECAS DA USP on September 6, 2007

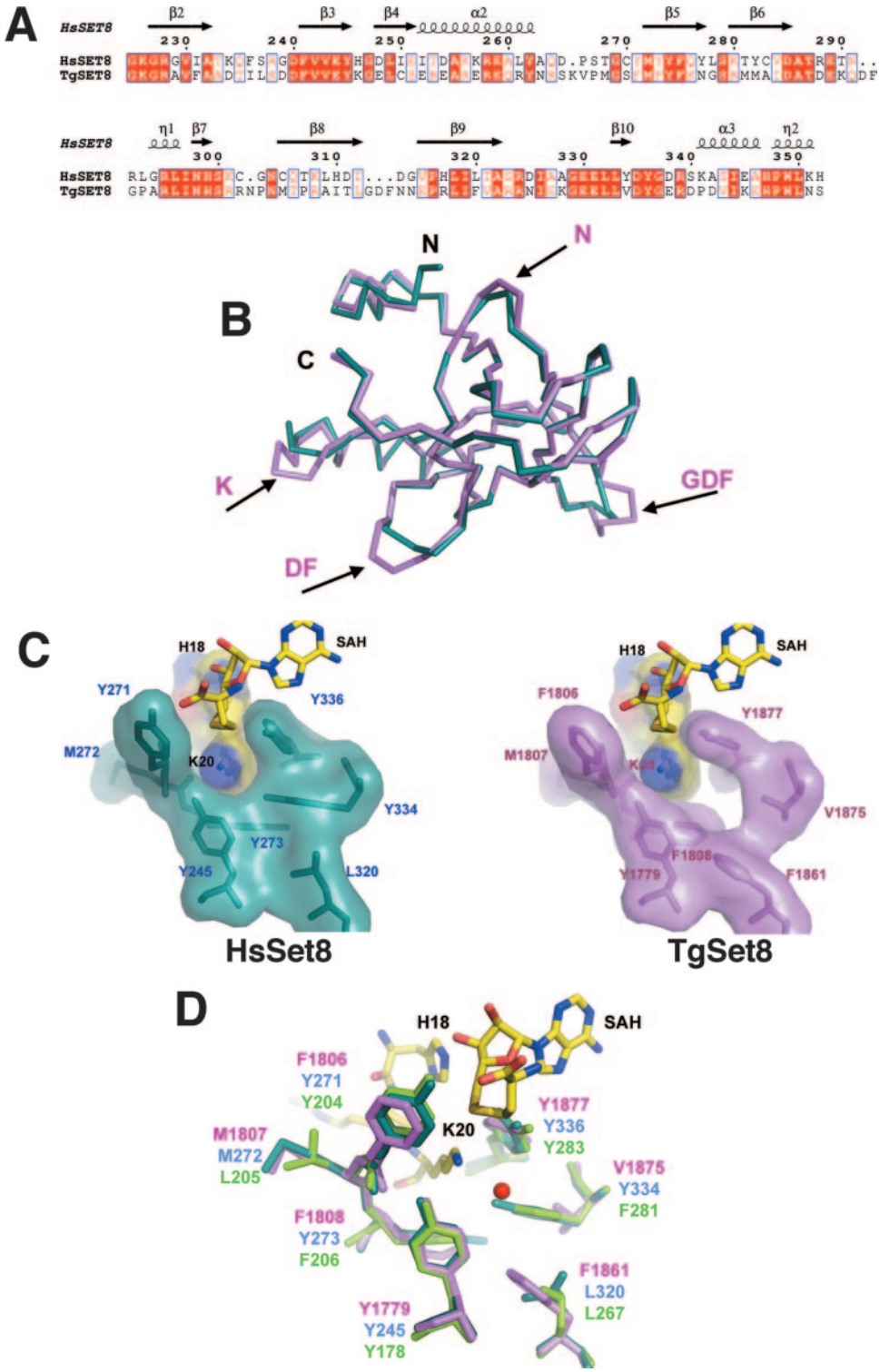

FIG. 3. Structural modeling of TgSet8ΔN5(1759-1893). (A) Primary sequence alignment of HsSet8(225-352) and TgSet8ΔN5(1759-1893) used for modeling with the program Modeler. The secondary-structure element annotations have been extracted from the HsSet8 1zkk Protein Data Bank structure (8). The image shown was produced with the program ESPRIT (14). (B) Superposition of the three-dimensional SET domains of HsSet8 (blue, 1zkkA) and the TgSet8ΔN5 Modeler model (pink). The TgSet8ΔN5 insertion sequences are indicated by arrows and the one-letter amino acid code. (C) The geometry and molecular environment of the lysine 20 binding site are shown for HsSet8 and TgSet8. (D) HsSet8 (blue), TgSet8 (pink), and DIM-5 (green) lysine 20 binding site residue superposition. The water molecule (red) belongs to the HsSet8 Protein Data Bank structure (1zkk).

Downloaded from mcb.asm.org at SISTEMA INTEGRADO DE BIBLIOTECAS DA USP on September 6, 2007

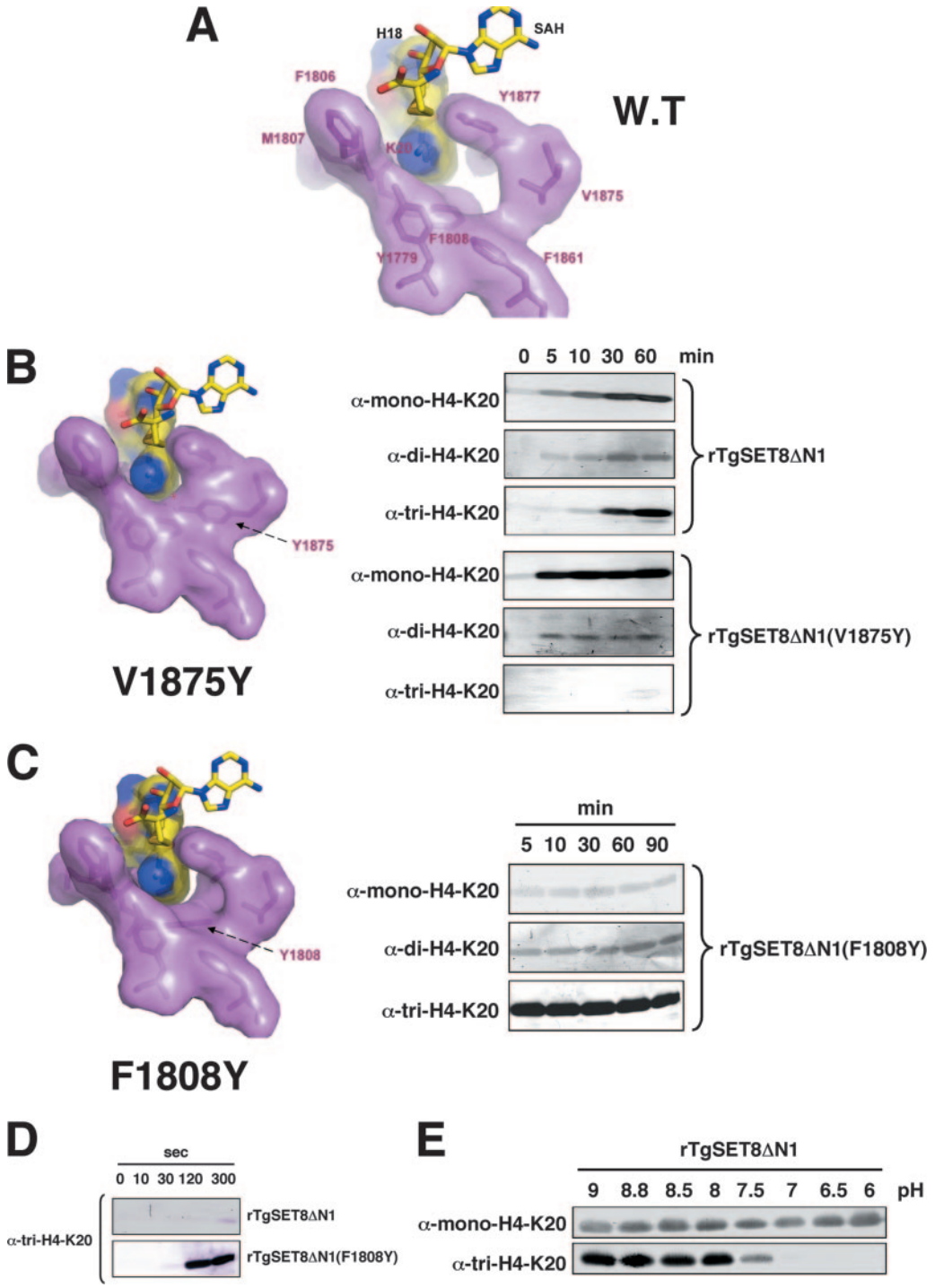

FIG. 4. Structural features of the TgSet8 catalytic site. The geometry and molecular environment of the lysine 20 binding site of wild-type (W.T.) (A) and mutant (B and C) TgSet8 are shown. (B) Time course HMTase assays of mutant TgSet8ΔN1(V1875Y) versus wild-type TgSet8 with recombinant His_6-H4 and analysis by Western blotting. A weak H4K20me2 signal is observed with long exposure times. (C and D) Time course HMTase assays of mutant TgSet8ΔN1(F1808Y) versus wild-type TgSet8 with recombinant His_6-H4 and analysis by Western blotting. (E) Influence of pH on the multiplicity of TgSet8ΔN1 on a His_6-H4 substrate.

entrance into and exit from the channel. In other words, the mutation may cause the lysine to be trapped inside the channel until it gets fully methylated.

For methylation to take place, the lysine side chain must be deprotonated. Several studies have assumed that Set8 relies upon the small but rapidly exchanging population of deprotonated target lysines (46). We then examined the pH dependence of TgSET8. Whereas TgSet8ΔN1 is able to monometh-

Downloaded from mcb.asm.org at SISTEMA INTEGRADO DE BIBLIOTECAS DA USP on September 6, 2007

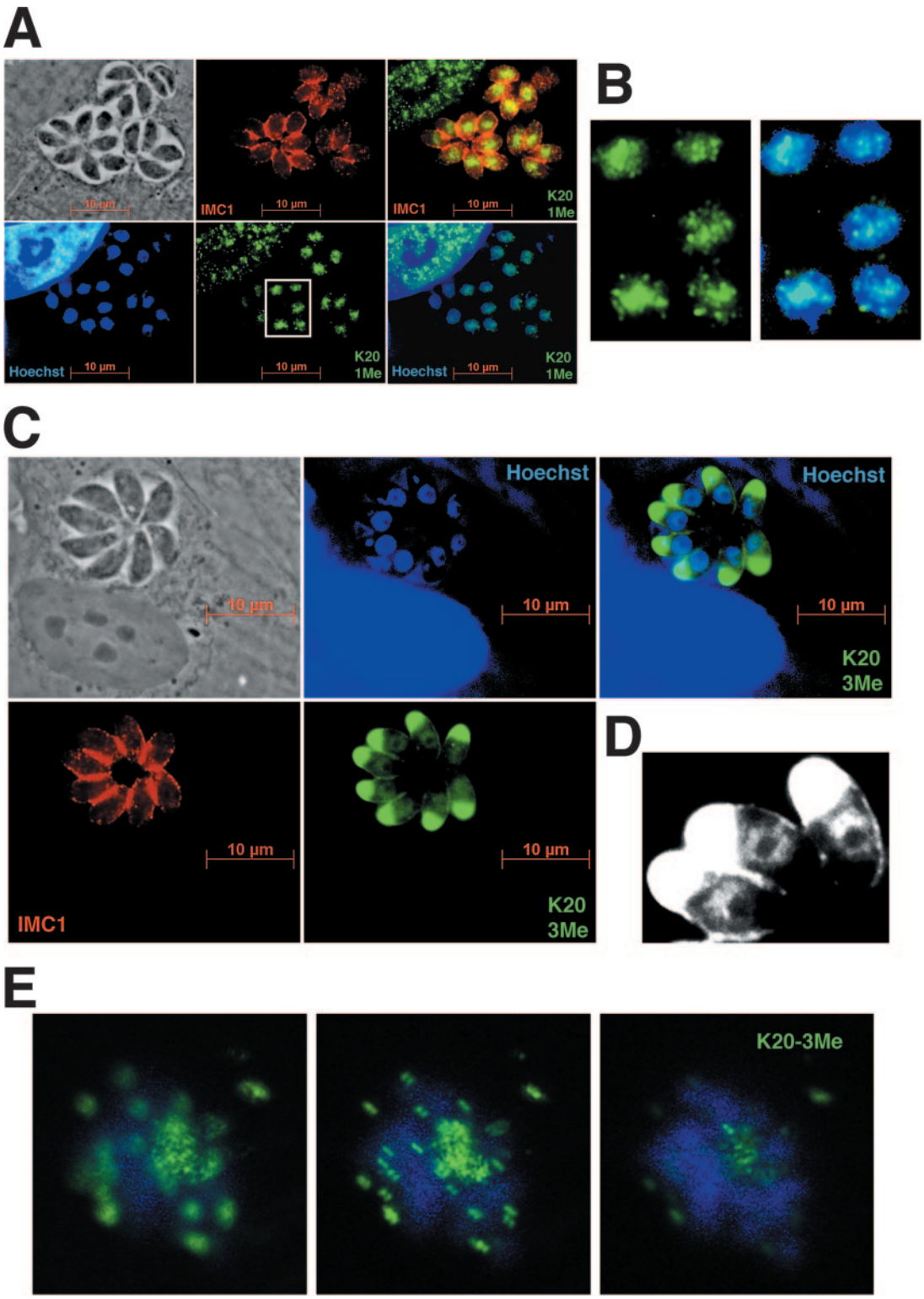

FIG. 5. H4K20me1 and H4K20me3 mark apicomplexan heterochromatin domains. (A) Costaining with anti-H4K20me1 antibody (green), anti-IMC1 antibody (red), and Hoechst 33258 (blue) of human fibroblast cells infected with *T. gondii* strain RH (tachyzoites). (B) Nuclear areas marked by H4K20me1 at a higher magnification. (C) Costaining with anti-H4K20me3 antibody (green), anti-IMC1 antibody (red), and Hoechst 33258 (blue) of human fibroblast cells infected with *T. gondii* strain RH (tachyzoites). (D) Nuclear areas marked by trimethyl H4K20me3 at a higher magnification. The cross-reactions at the apical end of *Toxoplasma* cells are frequently observed with antibodies raised against any trimethylated lysine residue. (E) Schizont stage *P. falciparum* parasites (strain 3D7) costained with anti-H4K20me3 antibody (green) and Hoechst 33258 (blue).

Downloaded from mcb.asm.org at SISTEMA INTEGRADO DE BIBLIOTECAS DA USP on September 6, 2007

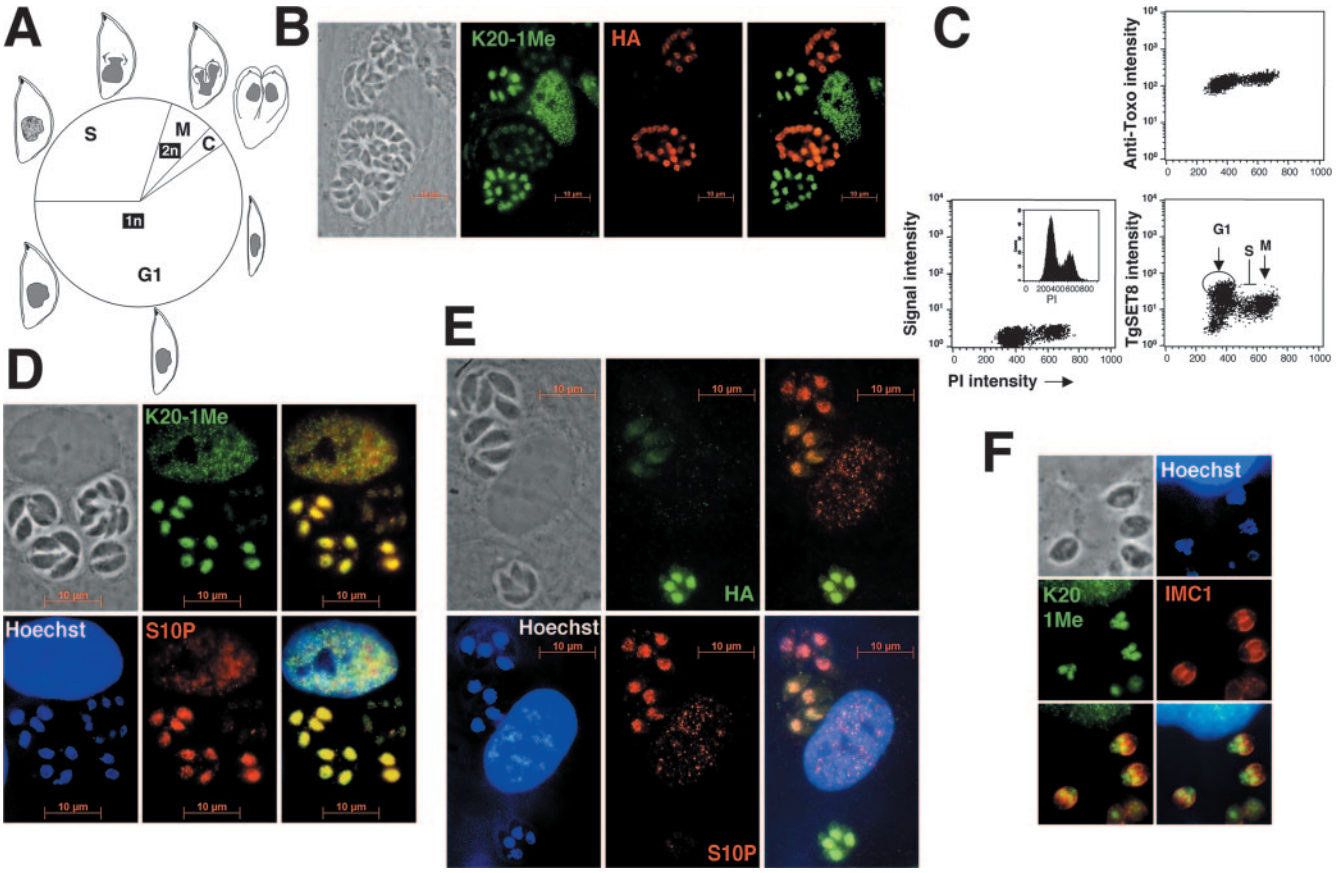

FIG. 6. The H4K20me1 marker is cell cycle regulated. (A) *T. gondii* cell cycle scheme. S, S phase; M, mitosis; C, cytokinesis. (B) Costaining with anti-HA antibody (red) and anti-H4K20me1 antibody (green) of human fibroblast cells infected with transgenic *T. gondii* strain RH::HA-Flag–TgSet8. (C) Fluorescence-activated cell sorter analysis of HA-Flag–TgSet8ΔN1 protein level in relation to the cell cycle. Tachyzoites were labeled with anti-HA and anti-*Toxoplasma* antibodies. DNA contents were detected with propidium iodide (PI). The intensity of the antibody fluorescence signal is plotted against the propidium iodide signal. The circle indicates an increase in the intensity of TgSet8ΔN1 expression in the tachyzoite G_1 phase. (D) Costaining with anti-H3S10ph antibody (red), anti-H4K20me1 antibody (green), and Hoechst 33258 (blue) of human fibroblast cells infected with *T. gondii* strain RH. (E) Costaining with anti-H3S10ph antibody (red), anti-HA antibody (green), and Hoechst 33258 (blue) of human fibroblast cells infected with strain RH::HA-Flag–TgSet8. (F) Costaining with anti-IMC1 antibody (red), anti-H4K20me1 antibody (green), and Hoechst 33258 (blue) of human fibroblast cells infected with *T. gondii* strain RH (tachyzoites in mitosis).

ylate lysine 20 of histone H4 in a broad pH range (~6 to 9), its trimethylase activity only appears from pH 7.5 (Fig. 4E). We could hypothesize that the second and third K20 deprotonation processes, necessary for full trimethylation to carry on, require pH-dependent deprotonations of active-site residues. Taken together, these observations suggest that several residues forming the substrate-specific channel play an important role in the methylation multiplicity ability of the SET domain by defining the geometry, size, and hydrophobic character of the lysine binding pocket.

H4K20me1 and H4K20me3 mark heterochromatic regions in *Apicomplexa*. We next turned our attention to how H4K20 mono-, di-, and trimethylations are distributed in *T. gondii*, *N. caninum*, and *Plasmodium falciparum* parasites by using specific antibodies and confocal fluorescence microscopy. H4K20me1 antibodies stained *Toxoplasma* and *Neospora* chromatin with a broad nuclear distribution (Fig. 5A; see Fig. S3A in the supplemental material). At higher magnification, H4K20me1 staining showed a punctate pattern spread throughout the nucleus, most likely the pericentric heterochromatin (Fig. 5B; see Fig. S3B in the supplemental material). In contrast, asexual erythrocytic stages of *P. falciparum* exhibited a weak monomethylation signal (data not shown). So far, no dimethylation immunofluorescent signal—with any available antibodies—was detected in parasite nuclei (data not shown), while the modification was readily visible by Western blotting (Fig. 2A). H4K20me3 was detected in *Toxoplasma* and *Neospora* nuclei as a ring structure with an accumulation primarily at the topmost nuclear periphery which is characteristic of perinuclear heterochromatin (Fig. 5C and D; see Fig. S3C to E in the supplemental material). Indeed, punctate, electron-dense bands of heterochromatin were commonly visualized at the periphery of *T. gondii* parasite nuclei (see Fig. S3F in the supplemental material). Immunostaining of *P. falciparum* young and mature schizonts revealed that the trimethylated marker was highly concentrated at some discrete foci, often grouped in pairs around the nucleus, suggestive of a telomeric signal (13) (Fig. 5E). Consistent with our data, the telomeres of *P. falciparum* were recently localized in the periphery of the nucleus, whereas acetylated H4 was found to be restricted to the center of the nucleus (see Fig. 3 in reference 13 and Fig. S3G in the supplemental

Downloaded from mcb.asm.org at SISTEMA INTEGRADO DE BIBLIOTECAS DA USP on September 6, 2007

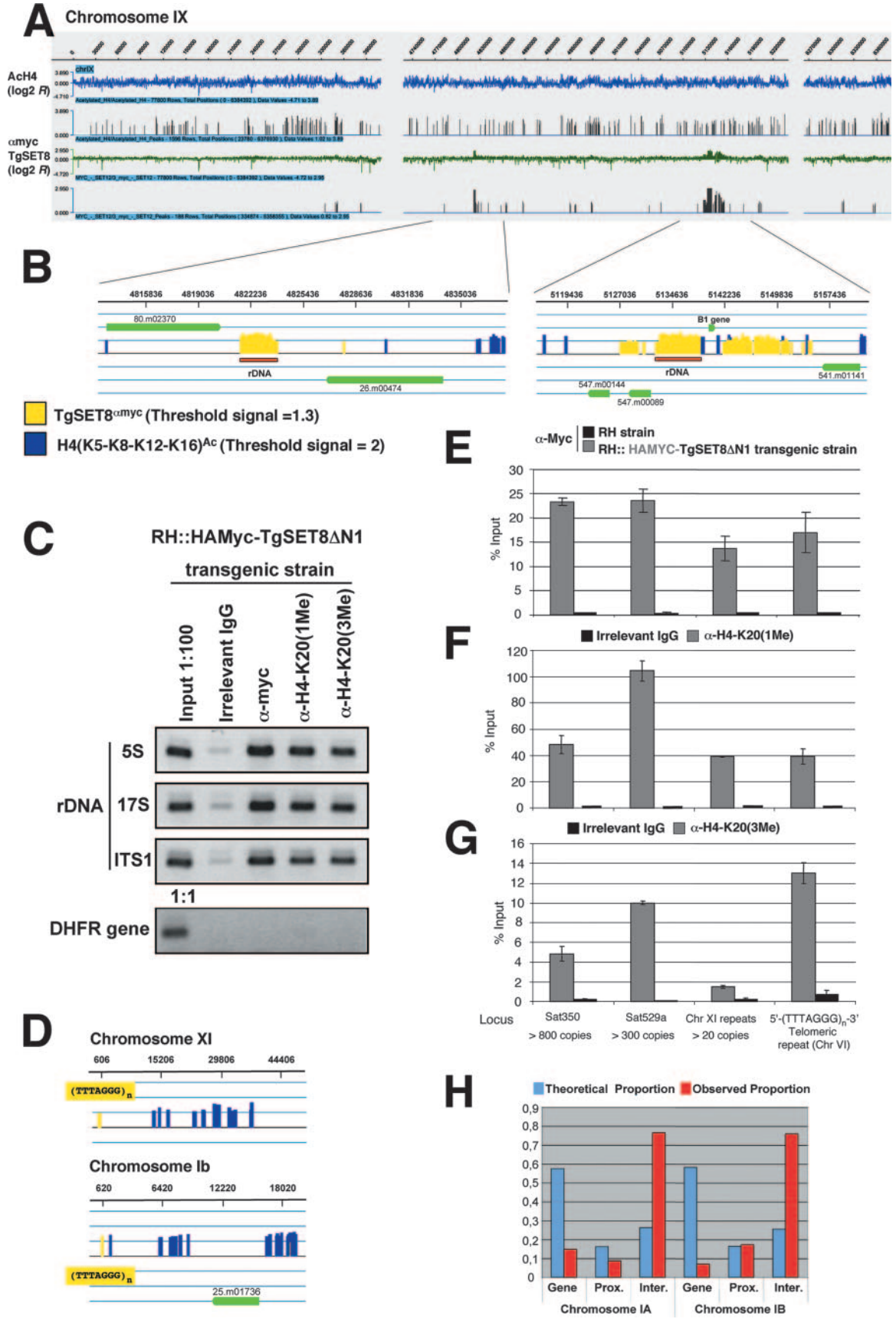

Downloaded from mcb.asm.org at SISTEMA INTEGRADO DE BIBLIOTECAS DA USP on September 6, 2007

material). These data are suggestive but not conclusive. Indeed, Hoechst DNA staining does not have sufficient resolution—because of the tiny nuclei of apicomplexans—to support unequivocal colocalization of the markers with the chromatin domain. On the other hand, ChIP analysis (see below for details) verified that the enzyme and its markers colocalize at heterochromatin in *T. gondii*.

Relationship between H4-K20 monomethylation and cell cycle regulation in *Toxoplasma*. Constitutive heterochromatin is stably inherited and thus must contain one or more epigenetic markers to direct its maintenance during cell division. Since recent studies have reported that H4K20me1 decreases at mid-S phase and increases during mitosis whereas Set8 protein levels are steadily elevated through G_2 and peak during mitosis (31), we investigated whether H4K20me1 is cell cycle regulated in *T. gondii*.

While cell division occurs by binary fission in most organisms, including bacteria, plants, and animals, apicomplexan parasites divide by endodyogeny or schizogony from a single polyploid mother to produce two or more daughters, respectively (Fig. 6A) (38). Thus, the vast majority of parasitophorous vacuoles contain 2^n parasites, where n indicates the number of parasite divisions resulting in geometric expansion of clonal progeny that eventually leads to host cell rupture (~48 h postinfection by a single parasite) (17). Moreover, tachyzoite endodyogeny consists of a singular three-phase cell cycle composed of major G_1 and S phases with mitosis immediately following DNA replication (Fig. 6A). The G_2 phase is either very short or absent in these parasites (29).

As assessed by immunostaining, the level of H4K20me1 methylation fluctuates from vacuole to vacuole; some contain larger parasites (presumably just before and during mitosis) with heavily decorated nuclei, while others carry slimmer parasites associated with much weaker fluorescence signals (Fig. 6B and D). In contrast, the synchronously replicating parasites within a given vacuole display signals of similar intensities. These data argue for tight regulation of the enzyme and its activity during the tachyzoite cell cycle. As a control, other epigenetic markers, such as the histone H3K4me2 level, were not found to vary during cell cycle progression (data not shown).

We raised several antibodies which, although they specifically recognized recombinant rTgSet8 in vitro, exhibited a weak immunofluorescence signal in vivo (data not shown). Since we could not accurately monitor the turnover of the endogenous protein over the cell cycle, we ended up using the chimeric protein HA-Flag–TgSet8ΔN1 for the following analysis. As to the level of HA-Flag–TgSet8ΔN1 ectopically expressed in tachyzoites, variations between vacuoles and homogeneity within vacuoles were again observed, despite the use of a strong constitutive parasite promoter (*GRA1*, Fig. 1C). This implies that the degradation of the chimeric protein is cell cycle regulated (Fig. 6B). In the same line of results, the endogenous protein TgSet8 followed the same pattern of expression (data not shown). It is unclear if TgSet8 RNA is upregulated during cell cycle progression, but our results demonstrate that the turnover of the protein is tightly controlled, even when it is ectopically expressed.

Surprisingly, the pronounced increase in H4K20me1 methylation coincides with a decrease in TgSet8ΔN1 protein levels and vice versa (Fig. 6B). To characterize the dynamics of methylation during the cell cycle, we also examined HA-Flag–TgSet8ΔN1 protein levels in a parasite population by flow cytometry analysis (Fig. 6C). While the protein remained relatively constant across the cell cycle, we observed peak intensities associated with the G_1 phase parasite population. To then address whether the H4K20me1 level increases during mitosis and decreases in G_1, we used additional mitosis markers. The phosphorylation of serine 10 on histone H3 is acknowledged as a conserved epigenetic marker of mitosis in organisms ranging from ciliates to mammals (44, 45). With specific anti-H3S10ph antibodies, we showed first that this as-yet-unreported modification exists in *Apicomplexa* and second that it correlates with chromosome condensation during *T. gondii* tachyzoite division. At the end of mitosis, histone H3 is expected to be dephosphorylated, which is consistent with the weakness of the signals observed (Fig. 6D and E; data not shown). Finally, we confirmed that H4K20me1 peaks during mitosis simultaneously with H3S10ph (Fig. 6D; see Fig. S4A in the supplemental material), while TgSet8 is primarily expressed in G_1 and degraded in M phase (Fig. 6E; see Fig. S4B in the supplemental material). Moreover, we noticed that par-

FIG. 7. H4K20 methylation states index heterochromatin in *T. gondii*. (A) Representative view of *Toxoplasma* ChIP-on-chip analysis. High-resolution mapping of both myc-Set8 binding sites and acetylated histone H4 (K5, K8, K12, and K16) locations on chromosome IX. The blue (H4ac) and green (myc-TgSet8) lines plot the median logarithmic ratio ($\log_2 R$) of hybridization intensities in a 500-base window of genomic versus immunoprecipitated DNA. The *x* axis denotes the genomic position of each probe, and the *y* axis shows the normalized log ratio of Cy5 and Cy3 signals, and therefore the signal strength is represented by the height of the rectangle. The data were visualized by the SignalMap software (NimbleGen Systems, Inc.). (B) Close-up view of chromosome IX regions. The horizontal bars represent possible binding regions identified by the SignalMap software. The height of the bar is the signal strength of the probe. Thresholds of 1.3 and 2 were applied to myc-Set8 (yellow) and acetylated histone H4 (blue), respectively. rRNA gene loci are shown in red. Green boxes indicate ToxoDB gene annotations. The data were visualized by the GenoBrowser software. (C) Chromatin from *T. gondii* strain RH::HAMyc-TgSet8ΔN1 was immunoprecipitated with anti-myc, anti-H4K20me1, and anti-H4K20me3 antibodies; immunoprecipitated DNA was analyzed by PCR with specific primers selected in *T. gondii* rRNA gene loci (5S, 17S, and ITS1; see Table S1 in the supplemental material) and the gene for dihydrofolate reductase (DHFR) as a negative control. (D) Detailed view of myc-Set8 (yellow) and H4ac (blue) ChIP-on-chip data at the chromosome XI and Ib telomeric regions. (E to G) DNA obtained by ChIP was analyzed by real-time PCR with repeat-specific primer sets (see Table S1 in the supplemental material). These particular loci were chosen for study because their amplification by real-time PCR gave specific amplicons. Assays were done under conditions in which the product accumulated linearly with respect to the input DNA (see Materials and Methods in the supplemental material). Relative intensity is shown with standard deviations. Chromatin from *T. gondii* strain RH::HAMyc-TgSet8ΔN1 was immunoprecipitated with anti-myc (E), anti-H4K20me1 (F), and anti-H4K20me3 (G) antibodies. (H) Statistical analyses of the HAMyc-TgSet8ΔN1 ChIP signal repartition across chromosomes Ia and Ib (see Materials and Methods in the supplemental material). The enzyme is more frequently enriched in the intergenic region than within gene-rich and promoter-proximal regions. IgG, immunoglobulin G; Chr, chromosome.

Downloaded from mcb.asm.org at SISTEMA INTEGRADO DE BIBLIOTECAS DA USP on September 6, 2007

asites engaged in cytokinesis still exhibited significant levels of H4K20me1, indicating that the marker is epigenetically transmitted to the daughter cell (Fig. 6F). However, no obvious localization of TgSet8 to mitotic chromosomes was observed (data not shown), which is contrary to what has been described for its human counterpart (31).

H4K20 and H3K9 methylations: a linear pathway for heterochromatin assembly in *T. gondii*. To search for target DNA regions where the TgSet8 protein is associated, we performed a ChIP-on-chip genome-wide analysis with chromatin from tachyzoite cells. We performed a ChIP experiment with a myc antibody and a stable transgenic parasite line expressing HAMyc-TgSet8ΔN1; we prepared amplicons and applied these amplicons to *T. gondii* full-genome oligonucleotide arrays (NimbleGen Systems, Inc.). Simultaneously, ChIP-on-chip analysis was also performed with antibodies recognizing very abundant chromatin landmarks like acetylated histone residues (e.g., acetylated histone H4 [K5-K8-K12-K16]), which possibly could identify the boundaries of euchromatin domains. We noted that the great majority of HAMyc-TgSet8ΔN1 binding sites were spaced far from each other (Fig. 7A). However, occasionally there were small chains (typically two or three peaks or chains) of binding sites spaced <1 kb from each other. Importantly, TgSet8 binding sites are prominently localized in hypoacetylated histone H4-enriched regions, suggesting that the enzyme preferentially targets heterochromatin domains (Fig. 7A). Moreover, the enzyme is predominantly enriched within intergenic regions (Fig. 7H; see Fig. S8 in the supplemental material).

First, our ChIP-on-chip data reveal that TgSet8 binds specifically to rRNA gene loci (Fig. 7B). In vertebrates, at the onset of mitosis, the nucleolus disintegrates and rRNA gene transcription ceases. Mitotic silencing of rRNA gene transcription occurs from prophase to telophase. In higher eukaryotes, the rRNA gene copies are clustered and distributed in active and silent nucleolar organizing regions (36). *T. gondii* rRNA gene copies are mono- and trimethylated at H4K20, and concurrently we detected the presence of the enzyme TgSet8 at these loci (Fig. 7B and C). This may explain how the epigenetic state of a given silent rRNA gene is propagated to daughter cells. In higher eukaryotes, the relative amounts of active and silent rRNA genes are maintained independently of transcriptional activity, suggesting that these chromatin states must be maintained throughout the cell cycle and propagated from one cell generation to the next (7).

In addition to rRNA gene loci, TgSet8 binds to several DNA repeats located near the telomeres but also widely dispersed along the *T. gondii* chromosomes such as canonical $(TTTAGGG)_n$ telomeric repeats or satellite DNA such as Sat350 (ABGTg/TGR family) and Sat529a (5) (Fig. 7D). Several high-copy-number repeat elements (up to 800 copies per haploid genome) are located near the telomeres but also along other regions in the largest *Toxoplasma* chromosomes (25, 32, 33).

We then confirmed by quantitative ChIP the distribution of TgSet8—observed by ChIP-on-chip analysis—at four repetitive-DNA-containing loci in a stable transgenic parasite line expressing HAMyc-TgSet8ΔN1. A robust anti-myc signal seen at these loci suggests that the enzyme methylates histone H4 at these chromosomal addresses (Fig. 7E). Consistent with these results, we found that H4K20me1 and H4K20me3 were both enriched at the loci whereas no enrichment was detected with the control antibody (Fig. 7F and G, respectively). Unfortunately, no significant enrichment of H4K20me2 was observed (data not shown). Whereas the H4K20me1 and H4K20me3 markers were significantly enriched, the repeats also contained H3K9 methylation as a second heterochromatic signature marker, although we observed a modest enrichment of the marker(s) (see Fig. S5 in the supplemental material). Overall, these studies suggest a functional synergy between the H3K9 and H4K20 methylation systems to establish and propagate apicomplexan heterochromatin and strongly support the idea that this pathway to silent chromatin is not restricted to metazoans, as previously thought.

DISCUSSION

Methyltransferase enzymes are key players in the regulation of chromatin modeling and associated properties, thereby driving numerous essential functions in most cells. In the present report, we characterize these molecules and activities in the large phylum of *Apicomplexa* parasites. These lower eukaryotes have developed a diverse panel of biological stages through their high capacity to differentiate, and epigenetics only begins to emerge as a strong determinant of their biology.

***Apicomplexa* parasites acquired Set8 HTMase homologues.** Whereas metazoans have at least two phylogenetically distinct H4K20 methyltransferases, Suv4-h20 and Set8/PR-Set7, the latter of which is considered an orphan, herein we bring the first evidence that the phylum of apicomplexan parasites harbors a single family of these enzymes phylogenetically and structurally related to Set8. We produced a TgSet8 SET domain model by the homology modeling technique and found that the overall architecture of the family-characterizing SET domain is conserved between *T. gondii* and human Set8 proteins. However, TgSet8 displays the unique feature of mono-, di-, and trimethylase activities, each of which is controlled at the single-amino-acid level. Remarkably, the V1875Y and F1808Y single-amino-acid changes are sufficient to abolish or increase the trimethylase activity, respectively. Additionally, in vivo-observed phenotypes of TgSet8 mutants are fully consistent with our in vitro data; tachyzoites that transiently express the mutant TgSet8ΔN1(F1808Y) protein no longer display an H4K20me1-associated signal but instead exhibit an increase in the H4K20 trimethyl signal (see Fig. S6A to D in the supplemental material). Such phenotypes also strongly argue that TgSet8 is the specific methylase to target H4-K20 in *T. gondii* cells. However, there are numerous SET domain enzymes in *Apicomplexa* whose histone lysine specificities are uncharacterized. So, we cannot exclude a priori the possibility that one or more of these SET enzymes are H4K20 specific and contribute to the establishment of the K20 methylation patterns observed in vivo. Examination of the fate of the H4K20 marker during differentiation from the rapidly dividing tachyzoite to the quiescent bradyzoite stage might also be informative. Our preliminary data on bradyzoites indicate that H4K20 is highly monomethylated, suggesting that TgSet8 is active in the quiescent cyst as well (see Fig. S7 in the supplemental material).

Set8 plays a pivotal role in heterochromatic histone methylation. While lysine methylations, in particular, H3K4, are widespread in eukaryotes (40), H4K20 methylation has initially

Downloaded from mcb.asm.org at SISTEMA INTEGRADO DE BIBLIOTECAS DA USP on September 6, 2007

emerged as a marker that preferentially indexes metazoan chromatin. HMTases that target repressive lysine positions (H3K9, H3K27, and H4K20) are absent from *S. cerevisiae*, strongly suggesting that the yeast lacks extensive heterochromatic domains and uses other repressive systems including SIR proteins to silence gene activity (23). It was then proposed that absence of the H4K20 marker could be linked to the more relaxed state of *S. cerevisiae* chromatin. However, the new information brought by the case of *Apicomplexa* parasites calls into question this idea since these parasites harbor H4K20 methylation while displaying a less condensed yeast-type chromatin. It therefore becomes questionable whether the evolution of this epigenetic marker is directly and only linked to the spatial packaging of nucleosomes.

Generally, heterochromatin is formed on highly repetitive satellite DNA in higher eukaryotes (16). In condensed chromosomes, satellite DNA is located in large clusters mostly in heterochromatic regions, near centromeres and telomeres, and sometimes interstitially (19). Metazoan heterochromatin is epigenetically defined by hypoacetylated histones H3 and H4 and methylated H3K9, H3K27, and H4K20. More specifically, H4K20 methylation states are signatures of constitutive heterochromatin that is typically devoid of gene expression (37, 39). We were tempted to speculate that repressive markers, such as histone H4K20 and H3K9 methylations, should also index *Toxoplasma* heterochromatin-embedded repetitive DNA sequences. By using ChIP in a cluster analysis representing *T. gondii* repetitive elements, we showed the selective enrichment of distinct H3K9 and H4K20 methylation markers across satellite DNAs and telomeres and also at rRNA gene loci for H4K20. These chromosomal regions are considered to be repressed, and such a state could be controlled by an H4K20 and H3K9 *trans*-tail histone code that specifically operates on parasite heterochromatin, as is known for mammals (37). Conversely, other repressive systems have been recently discovered to generate and maintain silent chromatin in apicomplexans. For example, a malaria gene homologous to yeast deacetylase Sir2 seems to be required for the establishment of a heterochromatin-like structure at the parasite telomeres, thereby promoting silencing of subtelomeric *var* genes (11, 13). Interestingly, we show that the trimethylated H4K20 epigenetic markers preferentially localize at subtelomeric domains in *P. falciparum* schizonts. Our data thus favor the idea that un- or hypoacetylated histones and methylated H4K20 (and presumably methylated H3K9) epigenetically define *Plasmodium*-silenced chromatin within the telomeres. On the other hand, Artur Scherf's laboratory recently showed that histone H4K16ac is highly enriched at the *var* 5′ untranslated region when it is transcriptionally active. And following parasite maturation, that area loses the acetylation marker (J. Lopez-Rubio, A. Gontijo, M. Nunes, R. Hernandez-Rivas, and A. Scherf, Mol. Parasitol. Meet. XVII, abstr. 3E, 2006). Moreover, Chookajorn et al. (4) reported recently that control of *var* gene transcription and antigenic variation is associated with a chromatin memory that includes H3K9me3 as an epigenetic marker. In metazoans, Set8 propagates the silent chromatin to newly synthesized DNA by marking H4K20 according to the map of unacetylated H4K16 on mitotic chromosomes (26, 31). Thus, these two markers could hypothetically negatively interact during parasitic cell cycle progression.

Conclusion. Here we present cumulative evidence that H4K20 is a major marker that exists in lower eukaryotes such as *Apicomplexa* parasites and that it controls, probably in concert with several other histone modification markers, the active or inactive status of the chromatin. In the light of our work and that of others, a central question remains how posttranslational histone modifications, in particular, H4K20 methylation, can regulate cell cycle progression in *Apicomplexa* parasites.

ACKNOWLEDGMENTS

Thanks go to J. C. Rice, G. E. Ward, and W. Bohne for antibodies and S. Yokoyama for vectors. We thank R. Ménard and W. J. Sullivan, Jr., for advice and helpful comments and Laurence Grossi and Karine Musset for technical help. We deeply thank P. Ortet for giving us the opportunity to use the "genome browser" software, which is still unpublished. Preliminary genomic and/or cDNA sequence data were accessed via http://ToxoDB.org (22).

M. A. Hakimi is supported by grants from CNRS (ATIP) and INSERM. Bastien Olivier is supported by an FRM fellowship. Genomic data were provided by the Institute for Genomic Research (supported by NIH grant AI05093) and by the Sanger Center (Wellcome Trust). Expressed sequence tags were generated by Washington University (NIH grant 1R01AI045806-01A1).

REFERENCES

1. **Aravind, L., and L. M. Iyer.** 2003. Provenance of SET-domain histone methyltransferases through duplication of a simple structural unit. Cell Cycle **2:**369–376.
2. **Beisel, C., A. Imhof, J. Greene, E. Kremmer, and F. Sauer.** 2002. Histone methylation by the Drosophila epigenetic transcriptional regulator Ash1. Nature **419:**857–862.
3. **Cheng, X., R. E. Collins, and X. Zhang.** 2005. Structural and sequence motifs of protein (histone) methylation enzymes. Annu. Rev. Biophys. Biomol. Struct. **34:**267–294.
4. **Chookajorn, T., R. Dzikowski, M. Frank, F. Li, A. Z. Jiwani, D. L. Hartl, and K. W. Deitsch.** 2007. Epigenetic memory at malaria virulence genes. Proc. Natl. Acad. Sci. USA **104:**899–902.
5. **Clemente, M., N. de Miguel, V. V. Lia, M. Matrajt, and S. O. Angel.** 2004. Structure analysis of two Toxoplasma gondii and Neospora caninum satellite DNA families and evolution of their common monomeric sequence. J. Mol. Evol. **58:**557–567.
6. **Collins, R. E., M. Tachibana, H. Tamaru, K. M. Smith, D. Jia, X. Zhang, E. U. Selker, Y. Shinkai, and X. Cheng.** 2005. In vitro and in vivo analyses of a Phe/Tyr switch controlling product specificity of histone lysine methyltransferases. J. Biol. Chem. **280:**5563–5570.
7. **Conconi, A., R. M. Widmer, T. Koller, and J. M. Sogo.** 1989. Two different chromatin structures coexist in ribosomal RNA genes throughout the cell cycle. Cell **57:**753–761.
8. **Couture, J. F., E. Collazo, J. S. Brunzelle, and R. C. Trievel.** 2005. Structural and functional analysis of SET8, a histone H4 Lys-20 methyltransferase. Genes Dev. **19:**1455–1465.
9. **Dillon, S. C., X. Zhang, R. C. Trievel, and X. Cheng.** 2005. The SET-domain protein superfamily: protein lysine methyltransferases. Genome Biol. **6:**227.
10. **Donald, R. G., D. Carter, B. Ullman, and D. S. Roos.** 1996. Insertional tagging, cloning, and expression of the Toxoplasma gondii hypoxanthine-xanthine-guanine phosphoribosyltransferase gene. Use as a selectable marker for stable transformation. J. Biol. Chem. **271:**14010–14019.
11. **Duraisingh, M. T., T. S. Voss, A. J. Marty, M. F. Duffy, R. T. Good, J. K. Thompson, L. H. Freitas-Junior, A. Scherf, B. S. Crabb, and A. F. Cowman.** 2005. Heterochromatin silencing and locus repositioning linked to regulation of virulence genes in Plasmodium falciparum. Cell **121:**13–24.
12. **Fang, J., Q. Feng, C. S. Ketel, H. Wang, R. Cao, L. Xia, H. Erdjument-Bromage, P. Tempst, J. A. Simon, and Y. Zhang.** 2002. Purification and functional characterization of SET8, a nucleosomal histone H4-lysine 20-specific methyltransferase. Curr. Biol. **12:**1086–1099.
13. **Freitas-Junior, L. H., R. Hernandez-Rivas, S. A. Ralph, D. Montiel-Condado, O. K. Ruvalcaba-Salazar, A. P. Rojas-Meza, L. Mancio-Silva, R. J. Leal-Silvestre, A. M. Gontijo, S. Shorte, and A. Scherf.** 2005. Telomeric heterochromatin propagation and histone acetylation control mutually exclusive expression of antigenic variation genes in malaria parasites. Cell **121:**25–36.
14. **Gouet, P., E. Courcelle, D. I. Stuart, and F. Metoz.** 1999. ESPript: analysis of multiple sequence alignments in PostScript. Bioinformatics **15:**305–308.
15. **Hackett, J. D., T. E. Scheetz, H. S. Yoon, M. B. Soares, M. F. Bonaldo, T. L. Casavant, and D. Bhattacharya.** 2005. Insights into a dinoflagellate genome through expressed sequence tag analysis. BMC Genomics **6:**80.

Downloaded from mcb.asm.org at SISTEMA INTEGRADO DE BIBLIOTECAS DA USP on September 6, 2007

16. **Henikoff, S.** 2000. Heterochromatin function in complex genomes. Biochim. Biophys. Acta **1470:**O1–8.
17. **Hu, K., T. Mann, B. Striepen, C. J. Beckers, D. S. Roos, and J. M. Murray.** 2002. Daughter cell assembly in the protozoan parasite Toxoplasma gondii. Mol. Biol. Cell **13:**593–606.
18. **Jenuwein, T., and C. D. Allis.** 2001. Translating the histone code. Science **293:**1074–1080.
19. **Jones, J. D., and R. B. Flavell.** 1983. Chromosomal structure and arrangement of repeated DNA sequences in the telomeric heterochromatin of Secale cereale and its relatives. Cold Spring Harbor Symp. Quant. Biol. **47**(Pt. 2)**:**1209–1213.
20. **Julien, E., and W. Herr.** 2004. A switch in mitotic histone H4 lysine 20 methylation status is linked to M phase defects upon loss of HCF-1. Mol. Cell **14:**713–725.
21. **Karachentsev, D., K. Sarma, D. Reinberg, and R. Steward.** 2005. PR-Set7-dependent methylation of histone H4 Lys 20 functions in repression of gene expression and is essential for mitosis. Genes Dev. **19:**431–435.
22. **Kissinger, J. C., B. Gajria, L. Li, I. T. Paulsen, and D. S. Roos.** 2003. ToxoDB: accessing the Toxoplasma gondii genome. Nucleic Acids Res. **31:**234–236.
23. **Kurdistani, S. K., and M. Grunstein.** 2003. Histone acetylation and deacetylation in yeast. Nat. Rev. Mol. Cell Biol. **4:**276–284.
24. **Martin, C., and Y. Zhang.** 2005. The diverse functions of histone lysine methylation. Nat. Rev. Mol. Cell Biol. **6:**838–849.
25. **Matrajt, M., S. O. Angel, V. Pszenny, E. Guarnera, D. S. Roos, and J. C. Garberi.** 1999. Arrays of repetitive DNA elements in the largest chromosomes of Toxoplasma gondii. Genome **42:**265–269.
26. **Nishioka, K., J. C. Rice, K. Sarma, H. Erdjument-Bromage, J. Werner, Y. Wang, S. Chuikov, P. Valenzuela, P. Tempst, R. Steward, J. T. Lis, C. D. Allis, and D. Reinberg.** 2002. PR-Set7 is a nucleosome-specific methyltransferase that modifies lysine 20 of histone H4 and is associated with silent chromatin. Mol. Cell **9:**1201–1213.
27. **Pradel, E., and J. J. Ewbank.** 2004. Genetic models in pathogenesis. Annu. Rev. Genet. **38:**347–363.
28. **Qian, C., and M. M. Zhou.** 2006. SET domain protein lysine methyltransferases: structure, specificity and catalysis. Cell. Mol. Life Sci. **63:**2755–2763.
29. **Radke, J. R., B. Striepen, M. N. Guerini, M. E. Jerome, D. S. Roos, and M. W. White.** 2001. Defining the cell cycle for the tachyzoite stage of Toxoplasma gondii. Mol. Biochem. Parasitol. **115:**165–175.
30. **Rayasam, G. V., O. Wendling, P. O. Angrand, M. Mark, K. Niederreither, L. Song, T. Lerouge, G. L. Hager, P. Chambon, and R. Losson.** 2003. NSD1 is essential for early post-implantation development and has a catalytically active SET domain. EMBO J. **22:**3153–3163.
31. **Rice, J. C., K. Nishioka, K. Sarma, R. Steward, D. Reinberg, and C. D. Allis.** 2002. Mitotic-specific methylation of histone H4 Lys 20 follows increased PR-Set7 expression and its localization to mitotic chromosomes. Genes Dev. **16:**2225–2230.
32. **Rocco, L., D. Costagliola, and V. Stingo.** 2001. (TTAGGG)n telomeric sequence in selachian chromosomes. Heredity **87:**583–588.
33. **Ruiz-Herrera, A., F. Garcia, C. Azzalin, E. Giulotto, J. Egozcue, M. Ponsa, and M. Garcia.** 2002. Distribution of intrachromosomal telomeric sequences (ITS) on Macaca fascicularis (Primates) chromosomes and their implication for chromosome evolution. Hum. Genet. **110:**578–586.
34. **Saksouk, N., M. M. Bhatti, S. Kieffer, A. T. Smith, K. Musset, J. Garin, W. J. Sullivan, Jr., M. F. Cesbron-Delauw, and M. A. Hakimi.** 2005. Histone-modifying complexes regulate gene expression pertinent to the differentiation of the protozoan parasite *Toxoplasma gondii*. Mol. Cell. Biol. **25:**10301–10314.
35. **Sanders, S. L., M. Portoso, J. Mata, J. Bahler, R. C. Allshire, and T. Kouzarides.** 2004. Methylation of histone H4 lysine 20 controls recruitment of Crb2 to sites of DNA damage. Cell **119:**603–614.
36. **Santoro, R.** 2005. The silence of the ribosomal RNA genes. Cell. Mol. Life Sci. **62:**2067–2079.
37. **Schotta, G., M. Lachner, K. Sarma, A. Ebert, R. Sengupta, G. Reuter, D. Reinberg, and T. Jenuwein.** 2004. A silencing pathway to induce H3-K9 and H4-K20 trimethylation at constitutive heterochromatin. Genes Dev. **18:**1251–1262.
38. **Sheffield, H. G., and M. L. Melton.** 1968. The fine structure and reproduction of Toxoplasma gondii. J. Parasitol. **54:**209–226.
39. **Sims, J. K., S. I. Houston, T. Magazinnik, and J. C. Rice.** 2006. A trans-tail histone code defined by monomethylated H4 Lys-20 and H3 Lys-9 demarcates distinct regions of silent chromatin. J. Biol. Chem. **281:**12760–12766.
40. **Strahl, B. D., R. Ohba, R. G. Cook, and C. D. Allis.** 1999. Methylation of histone H3 at lysine 4 is highly conserved and correlates with transcriptionally active nuclei in Tetrahymena. Proc. Natl. Acad. Sci. USA **96:**14967–14972.
41. **Sullivan, W. J., Jr., and M. A. Hakimi.** 2006. Histone mediated gene activation in Toxoplasma gondii. Mol. Biochem. Parasitol. **148:**109–116.
42. **Tanaka, Y., M. Tawaramoto-Sasanuma, S. Kawaguchi, T. Ohta, K. Yoda, H. Kurumizaka, and S. Yokoyama.** 2004. Expression and purification of recombinant human histones. Methods **33:**3–11.
43. **Templeton, T. J., L. M. Iyer, V. Anantharaman, S. Enomoto, J. E. Abrahante, G. M. Subramanian, S. F. Hoffman, M. S. Abrahamsen, and L. Aravind.** 2004. Comparative analysis of apicomplexa and genomic diversity in eukaryotes. Genome Res. **14:**1686–1695.
44. **Van Hooser, A., D. W. Goodrich, C. D. Allis, B. R. Brinkley, and M. A. Mancini.** 1998. Histone H3 phosphorylation is required for the initiation, but not maintenance, of mammalian chromosome condensation. J. Cell Sci. **111**(Pt. 23)**:**3497–3506.
45. **Wei, Y., C. A. Mizzen, R. G. Cook, M. A. Gorovsky, and C. D. Allis.** 1998. Phosphorylation of histone H3 at serine 10 is correlated with chromosome condensation during mitosis and meiosis in Tetrahymena. Proc. Natl. Acad. Sci. USA **95:**7480–7484.
46. **Xiao, B., C. Jing, G. Kelly, P. A. Walker, F. W. Muskett, T. A. Frenkiel, S. R. Martin, K. Sarma, D. Reinberg, S. J. Gamblin, and J. R. Wilson.** 2005. Specificity and mechanism of the histone methyltransferase Pr-Set7. Genes Dev. **19:**1444–1454.
47. **Yin, Y., C. Liu, S. N. Tsai, B Zhou, S. M. Ngai, and G. Zhu.** 2005. SET8 recognizes the sequence RHRK20VLRDN within the N terminus of histone H4 and mono-methylates lysine 20. J. Biol. Chem. **280:**30025–30031.
48. **Zhang, X., H. Tamaru, S. I. Khan, J. R. Horton, L. J. Keefe, E. U. Selker, and X. Cheng.** 2002. Structure of the Neurospora SET domain protein DIM-5, a histone H3 lysine methyltransferase. Cell **111:**117–127.
49. **Zhang, X., Z. Yang, S. I. Khan, J. R. Horton, H. Tamaru, E. U. Selker, and X. Cheng.** 2003. Structural basis for the product specificity of histone lysine methyltransferases. Mol. Cell **12:**177–185.

Downloaded from mcb.asm.org at SISTEMA INTEGRADO DE BIBLIOTECAS DA USP on September 6, 2007